

RESEARCH ARTICLE

Effect of treated palm fibers on the mechanical properties of compressed earth bricks stabilized by alkali-activated binder-based natural pozzolan

Rolande Aurelie Tchouateu Kamwa^{1,2}  | Joseph Bikoun Mousi^{1,3} | Sylvain Tome^{1,2} | Juvenal Giogetti Deutou Nemaleu⁴  | Martine Gérard⁵ | Marie-Annie Ettoh² | Jacques Etame¹

¹Department of Civil Engineering, University Institute of Technology (IUT), University of Douala, Douala, Cameroon

²Department of Chemistry, Faculty of Sciences, University of Douala, Douala, Cameroon

³Department of Civil Engineering, Higher National Engineering Polytechnic School (HNPS), University of Douala, Douala, Cameroon

⁴Local Material Promotion Authority (MIPROMALO), Yaoundé, Cameroon

⁵Institut de minéralogie, de physique des matériaux et de cosmochimie (IMPMC), Sorbonne Université, Paris, France

Correspondence

Rolande Aurelie Tchouateu Kamwa, Department of Civil Engineering, University Institute of Technology (IUT), University of Douala, P.O. Box 8698 Douala, Cameroon.
Email: aurelietchouateu19@gmail.com

Abstract

The aim of this work is to study the influence of the palm fibers treated with soda hydroxide solution on the properties of the compressed earth bricks stabilized (CEBs) with alkali-activated binder. The improvement in their mechanical parameters is attributable with 15 wt.% of alkali-activated binder-based natural pozzolan. To achieve this objective, mortars composed of treated fibers at different levels (0.1, 0.2, 0.3, 0.4, and 0.5 wt.%) of lengths of 4 and 16 cm have been developed. These different mortars with and without fibers were subjected to mechanical (dry and wet compressive test, flexural test), physical (water absorption), mineralogical (XRD, FTIR), and microstructural (SEM/EDS) characterizations after 7 and 90 days. The results revealed that in general the incorporation of fibers improves the mechanical and physical properties of CEBs stabilized with 15 wt.% of alkali-activated binder. Furthermore, the X-ray diffraction analysis indicated that certain mineralogical phases of the raw materials dissolve during alkaline activation. The Fourier transform infrared spectra revealed the effectiveness of the fibers in sorption water molecules. Moreover, optical examination reveals that the binder utilized completely wraps the fibers. This demonstrates that the treated fibers function flawlessly as a filler in the matrix. At 90 days with the addition of 0.4 wt.% fibers, the maximum dry compressive strength and flexural strength values were 8.08 ± 0.40 and 5.8 ± 0.19 MPa, respectively. The stabilized earth bricks reinforced with 0.4 wt.% of palm fibers exhibited the mechanical properties values fitting the requirements of the materials candidate for the building construction applications especially as masonry bricks.

This is an open access article under the terms of the [Creative Commons Attribution](https://creativecommons.org/licenses/by/4.0/) License, which permits use, distribution and reproduction in any medium, provided the original work is properly cited.

© 2024 The Author(s). *International Journal of Ceramic Engineering & Science* published by Wiley Periodicals LLC. on behalf of the American Ceramic Society.

KEYWORDS

alkaline stabilization, building, earth brick, palm fibers

1 | INTRODUCTION

Nowadays, research in the field of eco-construction focuses on the recovery of local materials, such as earth, volcanic ash, and industrial waste; while improving their technological characteristics by adding Portland cement, lime, geopolymer binders or activated binder, natural and synthetic fibers. Many studies on the value of local raw materials in construction have identified stabilized compressed earth bricks (CEBs) with Portland cement and geopolymer binder or activated binder as a promising solution for sustainable construction in Cameroon and many other countries.^{1–3} Stabilized earth bricks using geopolymer binders or activated binder, while still rarely employed in industry, show physico-mechanical properties comparable to those stabilized with ordinary Portland cement.¹ Furthermore, these new materials enable increased recovery of local raw materials while using less energy consumption.^{2,4}

Previously, Aurelie and co-workers^{5,6} produced the CEBs stabilized by acid and alkaline binders-based natural pozzolan (PZ) and this study have shed light in the field of geopolymerization. These works demonstrate that natural PZ-based geopolymer binders are effective for stabilizing earth bricks. However, stabilized earth bricks using phosphate-based geopolymer exhibit good characteristics to those stabilized using alkaline-based geopolymer in terms of mechanical properties. This is because the natural PZ utilized as a precursor for the geopolymerization procedure is crystallized and more reactive in acidic than alkaline environments.⁷ However, the alkaline activator is eco-friendlier than phosphoric acid activator. In general, alkaline geopolymer binder is product derived from the activation of an amorphous aluminosilicate precursor by an alkaline solution. If the precursor is crystallized, it is called alkali-activated binders and in this case, the mechanical properties can be quite weak.

To overcome this, the use of sustainable and carbon footprint less vegetable fibers offers alternative ways for reinforcement and improvement the properties as well of CEBs stabilized using alkali-activated binders. From literature database, numerous studies demonstrated the effectiveness of adding vegetables fibers (date palm, hemp, corn, millet, oil palm, coconut, barley straw, jute, pineapple) in improving the properties of CEB.^{8–10}

Cameroon is situated in tropical area that is characterized by hot and humid climate. The country has several

agricultural firms with huge oil palm plantations. Annual production is estimated at 230,000 tons per year, which ranks the country 13th in the world in this field.¹¹ Oil palm plantations occupy more than 14 million hectares in the country's inter-tropical zone.⁹ Once renewed, the oil palm generates huge waste products such as the fibers that wrap around the trunk. For instance, its lignocellulose content makes it sustainable raw material to produce cost-effective and environment-friendly composite materials. By combining at least two types of immiscible materials that have good adhesion, a composite is formed with properties that the individual base materials do not have.

Palm fibers have recently attracted a great deal of interest in the synthetic insulation technology. They proved the ability to act as reinforcement agent for the brick-fiber matrices by improving the mechanical properties, thermal conductivity and energy efficiency of these composites during the heating process.^{12,13} However, to date the investigations on the use of palm fibers although its abundance, as fibers reinforcement within the alkaline geopolymer bricks and alkali-activated bricks is not yet widespread. Furthermore, past research has demonstrated that the using of geopolymer and activated materials would result in more environmentally responsible construction in the future. It is therefore essential to investigate the characteristics that can be used to improve the qualities of those materials. Based on these qualities, palm fibers appear to be one of the sustainable waste materials that can significantly improve the features of stabilized bricks. This work thus, focuses on the recovery of the oil palm fibers and their valorization in the reinforcement of CEBs stabilized by alkali-activated binder-based volcanic ash (PZ).

2 | MATERIALS AND METHODS

2.1 | Clay soil and natural pozzolan (volcanic ash)

The clayey soils (CS) used for the produced the compressed earth block were collected in the quarry neighboring at Dibamba, Littoral-Cameroon. Volcanic ash named in this study as natural PZ was previously described and characterized in detail.⁵ Both materials were oven-dried for 24 h at 105°C, crushed using a ball mill and a pulverization method. Afterward, the resulting powders were passed through the sieve having sized of 500 and 80 µm for clay

TABLE 1 Chemical composition of the clay soil and the natural pozzolan.

Chemical composition (wt.%)									
Oxides	SiO ₂	Al ₂ O ₃	CaO	Fe ₂ O ₃	Na ₂ O ₃	K ₂ O	MgO	P ₂ O ₅	TiO ₂
C	44.4	25.9	2.36	9.27	2.5	1.87	1.7	0.8	1.78
PZ	47.9	15.8	8.6	12.9	3.7	2.8	6.4	–	–

soil and natural PZ, respectively. The chemical composition in wt.% of the CS and the PZ was determined using XRF analysis and described in Table 1.

2.2 | Alkaline activator solution and palm fibers

The alkaline solution was made by combining sodium hydroxide and sodium silicate. Analytical grade sodium hydroxide in flake (98% purity) was used to prepare 10 M NaOH solution. After 24 h the NaOH solution in mass percentage (63.2% Na₂O and 18.4% H₂O) was mixed with commercial water glass (28.7% of SiO₂, 8.9% of Na₂O, and 62.4% of H₂O). The resulting solution in mass percentage (23.99% SiO₂, 23.84% Na₂O, and 52.17% H₂O) was maintained for 24 h before being used in the processing and fabrication of green samples according to the work of Tchouateu et al.¹⁴ and Koadri et al.⁹ respectively.

The fibers used in this work are derived from the leaves of a *monocotyledonous* plant in the *Arecaceae* family, specifically from the *Elaeis* genus (Figure 1A,B), harvested in palm farm neighboring at Dibombari, Littoral-Cameroon. Once the bio-waste had been collected, it was manually defibered using a metal comb (Figure 1B). The obtained fibers were treated in 2.5M of NaOH (for 7 h) to improve the adhesion of the matrix–fiber interface. Actually, the alkaline treatment of the bio-waste fibers was done following the process described by Ali et al.¹⁵ In their work focused on the hydrophobic treatment of natural fibers and their composites, the authors found that the nature of the surface and the hydrophobic character of natural fibers result in low mechanical qualities for the products, it is critical to treat these fibers to improve these capabilities. After the soda treatment, the fibers are saturated in an acidified solution (acetic acid), thoroughly rinsed with tap water to remove all residues of NaOH, air-dried for 24 h, and cut into two distinct lengths of 16 and 4 cm according to the statements described by Manniello et al.¹⁶ and Sharma et al.,¹⁷ respectively. They revealed that the aspect of the fibers impacts the mechanical properties of the products. They showed that the greater the length of the fiber, the more these properties increase. In the study of Manniello et al.,¹⁶ they varied the fiber length from 0 to 70 mm and

obtained a linear increase in tensile strength. This strength with 70 mm fibers is twice of the strength of the sample without fibers. The physical properties of palm fibers are 1.09–1.2 g/cm³ of density, 300–550 μm of diameter, and 0.5–1 m of length.

2.3 | Composite preparation

Table 2 describes the different mix proportions of clay soil, natural PZ, sodium silicate solution, and palm fibers used for the different composites. The unstabilized CEBs were made by uniaxial pressing at 8 MPa of the homogeneous mixture of CS, volcanic ash, and sodium silicate solution, with added fibers. The ratio of water and mass is fixed at 0.3.

For the formulation of stabilized earth bricks (CEBs0), the following process was used: powdered CS at 500 μm (85 % of total mix) and natural PZ at 80 μm (7.5 % of total mix) were manually mixed. Afterward, the alkaline activator solution (7.5 % of total mix) described in Section 2.2 was added, and the obtained mortar was further manually mixed for 5 min. Subsequently, the different products were obtained by compressing the mixture at room temperature (25°C ±1°C) with relative humidity levels average around 80% and a pressure of 8 Mpa, applied with 0.5 MPa ·s^{−1} using Cyber-plus progress 2000 KN-Matest press. The ratio liquid and solid (alkaline solution/natural PZ) is fixed at 1 following Equation (1):

$$\frac{\text{alkaline solution}}{\text{natural pozzolan}} = 1. \quad (1)$$

The production of composite matrices consists by compressing the prismatic form of mixing alkali activated mortar and various proportions of treated fibers from 0 to 0.5 wt.% at 1.5 cm in relation to the total thickness of samples. The specimens were labeled CEBs0, CEBs0.1, CEBs0.2, CEBs0.3, CEBs0.4, and CEBs0.5 (Table 2 and Figure 2). It is base of the previous study carried out by Zainate et al.⁹ and Malanda et al.¹⁷ on the composite materials that the proportions of fibers were chosen. At room temperature, two sets of compressed blocks form including cubic (4 × 4 × 4 cm³) and prismatic (4 × 4 × 16 cm³), were made using mechanical uniaxial press at 8 MPa. The obtained blocks were sealed in plastic bags at room temperature (25±1°C) before the curing regime at 7 and 90 days. By the end of the curing, the hardened samples were subjected to various tests.

The lignocellulose (wt.%) composition of treated palm fibers was assessed using Pycnolab laboratories chemical procedures. The detailed procedure was described by Elfaleh et al.¹⁸



FIGURE 1 Plant free of leaves around the trunk (a) and the leaves (b). Fiber collection (c), defibration (d), soda treatment (e), drying (f), and measurement (g).

TABLE 2 Composition (wt.%) of prepared samples.

Samples	CEB	CEBs0	CEBs0.1	CEBs0.2	CEBs0.3	CEBs0.4	CEBs0.5
Clays soil	100	85	84.9	84.8	84.7	84.6	84.5
Natural pozzolan	0	7.5	7.5	7.5	7.5	7.5	7.5
Sodium silicate	0	7.5	7.5	7.5	7.5	7.5	7.5
palm fibers	0	0	0.1	0.2	0.3	0.4	0.5

TABLE 3 Composition in grams of basic materials for compressed earth brick (4×4×16 cm).

Samples	CEB	CEBs0	CEBs0.1	CEBs0.2	CEBs0.3	CEBs0.4	CEBs0.5
Clays soil	250	212.5	212.3	212.1	211.9	211.7	211.4
Natural pozzolan	0	18.75	18.75	18.75	18.75	18.75	18.75
Sodium silicate	0	18.75	18.75	18.75	18.75	18.75	18.75
Palm fibers	0	0	0.2	0.4	0.6	0.9	1.1

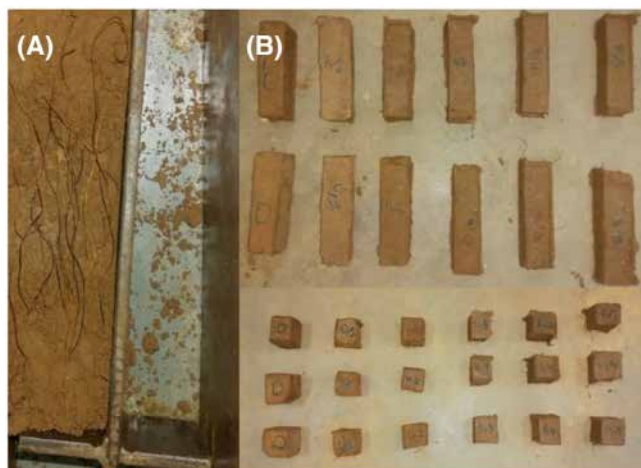
Abbreviations: CEB, Compressed earth brick made with 100 wt.% of clay soil; CEBs0, stabilized compressed earth bricks made with 85 wt.% of clay soil, 7.5 wt.% of natural pozzolan, and 7.5 wt.% of sodium silicate solution; CEBs0.1 to 0.5, stabilized compressed earth brick with 84.9–84.5 wt.%, 7.5 wt.% of natural pozzolan, and 7.5 wt.% of sodium silicate solution and 0.1–0.5 wt.% of palm fibers.

TABLE 4 Physical properties of clay soil (CS): Granular distribution (%) and Atterberg limits.

Sample	Gravel $\Phi > 2 \text{ mm}$	Sand $2 > \Phi > 0.02 \text{ mm}$	Silt $0.02 > \Phi > 0.002 \text{ mm}$	Clay $\Phi < 0.002 \text{ mm}$	Liquid limit	Plastic limit	Plasticity index	Plasticity domain
CS	0.29	74.22	2.94	22.54	32.11	43.58	11.47	Medium plastic

TABLE 5 Chemical characteristics of non-treated and treated palm fibers.

Constituents (wt.%)			
Non-treated palm fiber	Lignin	Hemicellulose	Cellulose rest
	30.5	20	46.8
Treated palm fiber	15.1	9	40 2.6

**FIGURE 2** Representative images of the arrangement of palm fibers (A) and different bricks (B).

2.4 | Characterization of raw material and composite structures

The different fractions of used CS were evaluated by the sedimentation techniques for fine particles according to ASTM D79280 standard.¹⁹ The workability of the soils under the Atterberg limit which is the difference between the liquid limit and the plastic limit of the same material was done by determining plasticity index values following ASTM D43180 standard.²⁰ The potential crystalline phases within the raw materials and the produced bricks were evaluated through powder X-ray diffraction (XRD) techniques through the Brucker-AXS D8 Debye-Scherrer type (Cu K α , $\lambda = 1.5418$ Å) 2θ in range 5°C – 70°C . The phase's identification was carried out using HighScore Plus software.

Fourier transform infrared (FTIR) analysis was performed to identify the various functional groups found in these samples. The KBr technique was used to record infrared spectra using a Bruker Vertex 80v spectrometer. This was done with a resolution of 2 cm^{-1} and 16 scans of the pellet from each sample. Each pellet was made by combining roughly 1.2 mg of the material with approximately 200 mg of KBr.

The morphological features of the specimens without and with fiber were observed using a Jeol XFlash 6160 Bruker scanning electron microscope (SEM) equipped

with energy dispersive X-ray spectroscopy (EDS). The samples were coated with a thin layer of gold to make them measurable under the microscope.

Each various mechanical and physical tests mentioned below are carried out on three samples.

The mechanical properties of earth bricks, including three-point bending test and compressive strengths (Figure 3A,B), were tested on wet and dry specimens with the loading rate of 5 mm/s using a compression test machine from Impact Test, UK with a maximum load capacity of 250 KN. The bending test is carried out on the $4 \times 4 \times 16\text{ cm}^3$ samples and the dry and wet compressive strengths on the $4 \times 4 \times 4\text{ cm}^3$ samples. Mean values and standard deviation were calculated using four representative samples for each formulation. These mechanical tests were performed according by the ASTM C642-06 standard.

Physical properties, including water absorption, were assessed on three samples of $4 \times 4 \times 4\text{ cm}^3$. For the water absorption ($W\%$) and wet strengths tests, 7 and 90 days aged samples were dried and weighted at room temperature ($25 \pm 1^\circ\text{C}$ with relative humidity levels average around 80%) until constant mass before being immersed in water at room temperature ($25 \pm 1^\circ\text{C}$) for 48 h. In terms of water absorption, after removing the water sample, the mass of the wet samples (M_w) was weighed and compared to the mass of the dry samples (M_d) using the ASTM C642-06 standard. The water absorption rate is given by the following equation:

$$W(\%) = \left(\frac{M_w - M_d}{M_d} \right) \times 100. \quad (2)$$

3 | RESULTS AND DISCUSSION

3.1 | Characterization of basic materials

Figure 3A,B displays the diffractogram patterns of clay soil (CS) and natural PZ. The diffractogram of CS shows that it is essentially composed of kaolinite (PDF-Nr. -000010527), quartz (PDF-Nr. -010741811), goethite (PDF-Nr. -010771060), and microcline (PDF-Nr. -000190926).

As it can be seen from Figure 4B, the natural PZ is predominantly made of phases that include: augite (PDF-Nr. -010781392), anorthite (PDF-Nr. -000411481), and hematite (PDF-Nr. -000240072). The absence of the 2θ region of the amorphous hump in the graph of PZ means that the natural PZ used is crystallized.

Table 4 shows physical properties of CS, principal material used for the manufacture of different CEBs. The particle size distribution showed that CS consisted of 0.29% gravel, 74.22% sand, 2.94% silt, and 22.54% clay. According to Atterberg, it is medium-plastic clay due to its plasticity

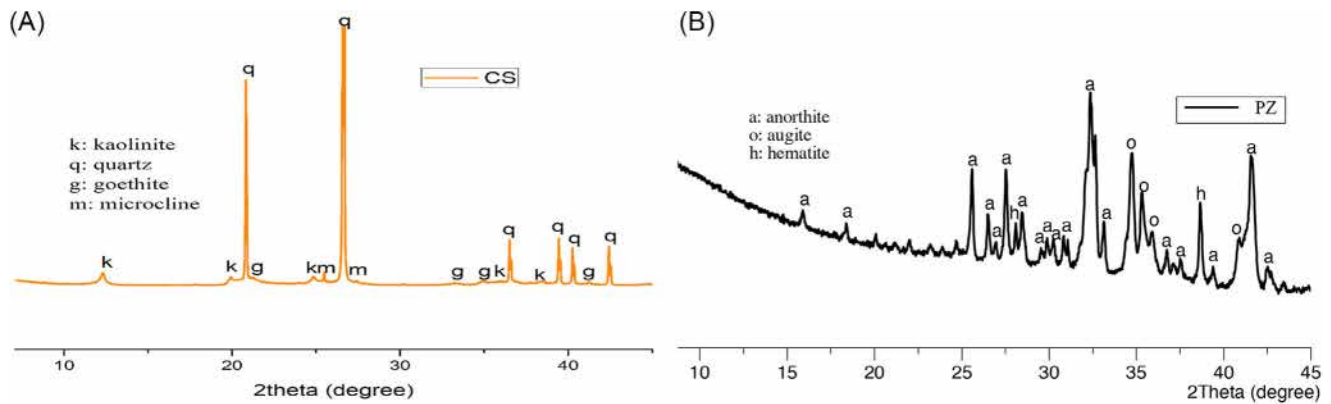


FIGURE 3 (A) XRD patterns of clay soil (CS), Cu⁰ theta. (B) XRD patterns of natural pozzolan (PZ), Cu⁰ theta. XRD, X-ray diffraction.

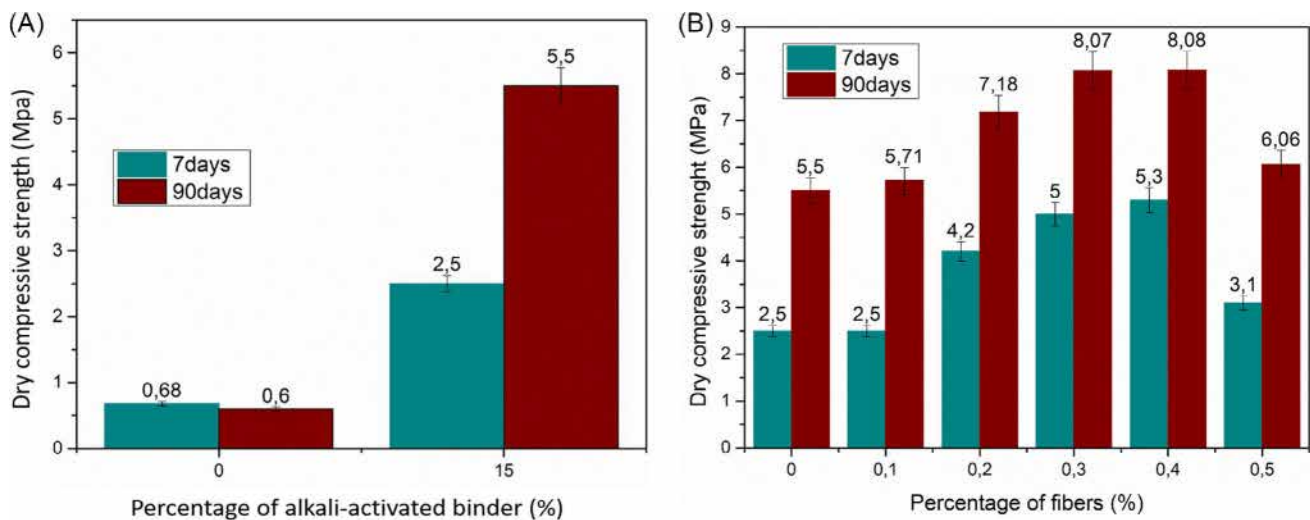


FIGURE 4 (A) Variations of dry compressive strength with alkali-activated binder and curing time. (B) Variations of dry compressive strength with palm fibers and curing time.

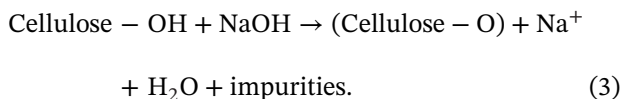
index ranges between 7 and 17. Furthermore, the classification of soils according to their nature, based on the particle size distribution of the sample and its plasticity index (11.47) presented in Table 4 categorized the used clay as type B5 (acceptable clay soil).²¹

3.2 | Chemical composition of palm fiber

The properties of natural fibers, their mechanical capabilities, and weak resistances are influenced by their chemical composition. The chemical composition of palm fibers used in this study is mentioned in Table 5. Non-treated palm consisted of cellulose (46.8%), hemicellulose (20%), and lignin (30.5%). After cellulose, lignin, which is the second most abundant renewable organic substance in this palm fiber. However, the presence of a sufficient amount of cellulose increases the strength of the fibers, while the

presence of lignite, due to its hydrophobicity, provides them water resistance, rigidity, and good hardness.^{22,23} However, plant fibers have certain drawbacks when combined with polymers. The presence of hydroxyl groups in lignocellulose, plant fibers are hydrophilic, making them incompatible with hydrophobic thermoplastics and prone to moisture damage.¹⁸ These limitations pose challenges for using plant fibers as polymer reinforcement. To improve adhesion between fibers and the polymer matrix and reduce moisture absorption, surface modifications are typically required. It is the reason of the use of alkaline (NaOH) treatment in this context to enhance fiber-matrix compatibility and improve composite quality.^{9,24} As the values mentioned in Table 3, alkaline treatment considerably reduced the percentage of lignin (30.5%–15.1%) and hemicellulose (20%–9%). The weak reduction of cellulose percentage (from 46.8% to 40%) resulted from the alkaline treatment that triggered the reaction of the fiber's hydroxyl

functions ($-\text{OH}$) of cellulose with acetyl groups ($-\text{COCH}_3$) to give the fiber a hydrophobic surface.²⁵ The reaction of NaOH with cellulose can be represented as follows:



3.3 | Mechanical characterization of composite materials

3.3.1 | Dry compressive strength

The compressive strength test was performed after 7 and 90 days of curing. The results obtained from the dry compression test as a function of the alkali-activated binder percentage (0 and 15 wt.%) and curing days (7 and 90 days) are presented in Figure 4A. When curing time further increased from 7 to 90 days, a weak decrease in compressive strength was observed for the unstabilized bricks. This decrease is due to the formation of crack in the unstabilized earth brick matrix with curing time. However, the adding of the alkali-activated binder (natural PZ + alkaline solution) and curing days directly affects the compressive strength performance of CEBs. With the addition of 15 wt.% of the alkali-activated at 90 days the compressive strength of bricks considerably increased. At 7 days, the values were 0.68 ± 0.03 and 2.5 ± 0.12 MPa for bricks containing 0 and 15 wt.%, respectively. Further curing up to 90 days induced the rise of the compressive strength up to 5.5 ± 0.27 MPa for bricks made with 15% alkali-activated binder while those made without the alkaline binder still close to 0.6 ± 0.03 MPa. This demonstrates that the addition of alkaline binder and the curing seemed beneficial for the compressive strength improvement of the earth bricks.

Figure 5B presents the compressive strengths behavior of the stabilized bricks reinforced with/without the treated fiber at 7 and 90 days. From Figure 5B, the curing time combined with the addition of the fiber up to 0.4 wt.% positively affected the compressive strength behavior of the produced material. This increase in compressive strength is due to the synergetic action of the formation of alkali-activated binders within the matrices and which strengthened with time, and the role played by the fibers as a reinforcement taking over the forces transmitted to the clay soil—alkali-activated binder matrix. However, the addition of 0.5 wt.% of fibers induced a slight compressive strength. Considering the hydrophilic nature and as well the wettability of the fibers, more content tends to delay the release water rate during the curing process inducing the weak bonding between the fiber and components within the matrices. This results in the decreasing trend observed of the com-

pressive strength (Figure 4B).^{26,27} In addition, the matrix formed by the fibers would no longer be in sufficient contact with the clay-binder matrix. Optimum dry compressive strength is achieved for an optimal proportion of 0.4 wt.% of fibers. At this rate and by comparing without fiber added, reinforced brick exhibited high compressive strength of 8.08 ± 0.40 MPa (Figure 4A,B). Furthermore, it is pointing noted that the ageing curing process to 7–90 days allowed the increasing of the compressive strength values at least 3 MPa for all the produced reinforced bricks (Figure 4B). This reflects the minor influence of the curing time on the treated palm fibers, with the corollary is the positive development of the strength due to the better bonding and cohesion between alkali-activated binder and other components. This phenomenon is also linked to the alteration over time of certain mineral phases present in natural PZs and CS (kaolinite, hematite, goethite, etc.) in an alkaline environment, which also leads to the formation of a polymeric network, once again contributing to the reinforcement of the alkali-activated binder.^{6,28,29}

3.3.2 | Wet compressive strength

Figure 5A,B shows the wet compressive strengths variation for the alkaline gel stabilization of bricks with palm fibers added at 7 and 90 days, respectively. Before the alkaline stabilization, the brick aged of 7 days presented weak wet compressive strength while those aged 90 days collapsed in water storage. The destruction is due to the fact that the capillarity in the fillers (clays and silt) within the used clay soil is still significant allowing the increasing rate of the absorbed water of the matrices.^{30,31} Besides, due to the linear swelling and/or shrinkage that occurs in the clay material (moderately plastic nature, Table 3), the number of open pores and cracks became great at 90 days rendering the brick more permeable in the presence of the liquid as water. Therefore, the combined action of pore capillarity rates and permeability flux in the water led to weakness and the destruction of the bonding network within the matrices. This resulted in the obtained brick with weak structure or even collapsed structure.

Similar phenomena and behavior above-mentioned in Section 3.3.1 were noted in the tested alkali-activated binder brick reinforced with the treated palm fibers (Figure 5). Thus, the wet compressive strength was positively affected, and the brick remained stability in humid areas. However, in the wet state, the compressive strength dropped to rate of 75% and 65% for the alkali-activated binder stabilized brick without fiber and fiber added, respectively. This meant that the addition of treated palm fibers has the advantage for water resistance of earth bricks stabilized by an alkali-activated binder. Furthermore, the

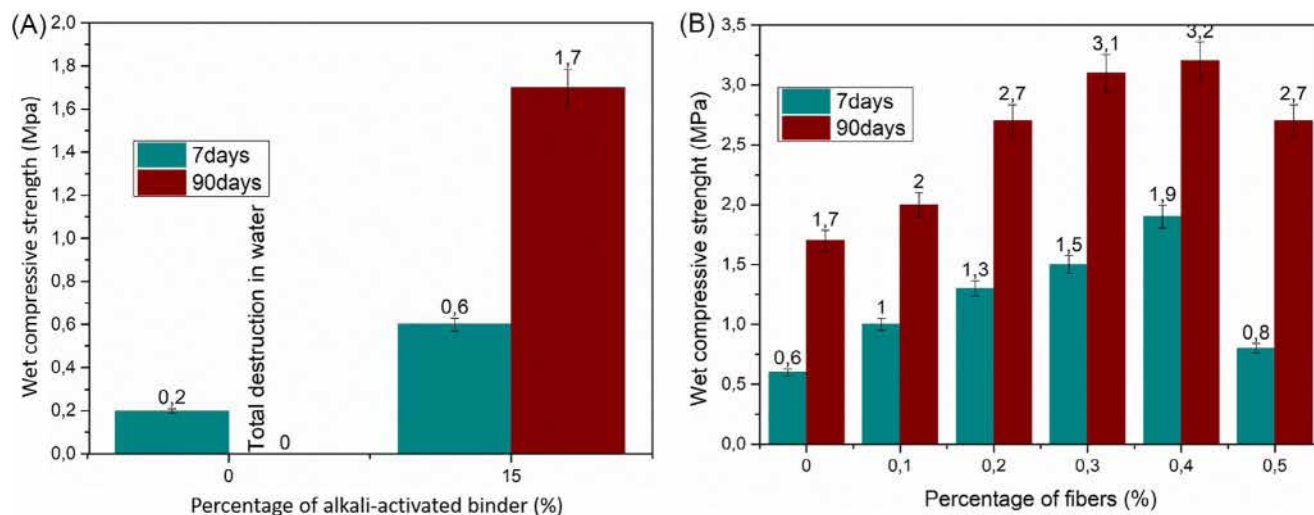


FIGURE 5 (A) Variations of wet compressive strength with alkali-activated binder and curing time. (B) Variations of wet compressive strength with palm fibers and curing time.

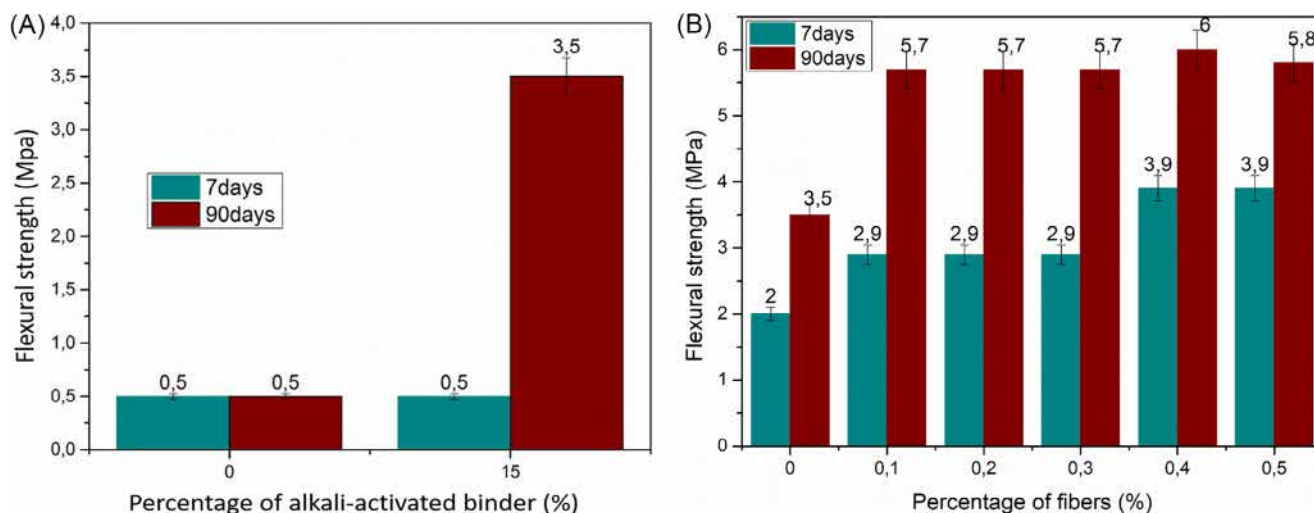


FIGURE 6 (A) Variations of flexural strength with alkali-activated binder and curing time. (B) Variations of flexural strength with palm fibers and curing time.

wet strength values of the fibrous composites obtained comply with that recommended by the XP 13-901 standard for construction with earth bricks (> 1 MPa), and the optimum values (3.2 ± 0.16 MPa) achieved for brick made with of 0.4 wt.% of fibers at 90 days.

3.3.3 | Flexural strength

The values of flexural strength of the different samples are reported in Figure 6A,B. From Figure 6A, both materials without and with the binder have the flexural strength value close at 0.5 MPa after 7 days of curing. This situation could be justified by the low reactivity of natural PZ in an alkaline environment.³² However,

after 90 days of curing, there was a considerable increase in flexural strength (Figure 6B), confirming the polymerization/polycondensation reaction that took place by progressive dissolution of the PZ particles to form the alkali-activated binder.³³ With regard to CEBs with alkali-activated binders, the improvement in their mechanical parameters is attributable to the production of alkali-activated binder networks that bond the particles together, thus making the samples compact and resistant with time.³⁴

At 90 days, the increasing of the palm fiber content up to 0.4 wt.% within the CEBs is beneficial in the flexural strength from 3.5 ± 0.17 to 6 ± 0.30 MPa. As with compressive strength, a 0.4% fiber addition rate yields the highest value. In this study, when the composites have a fibrous

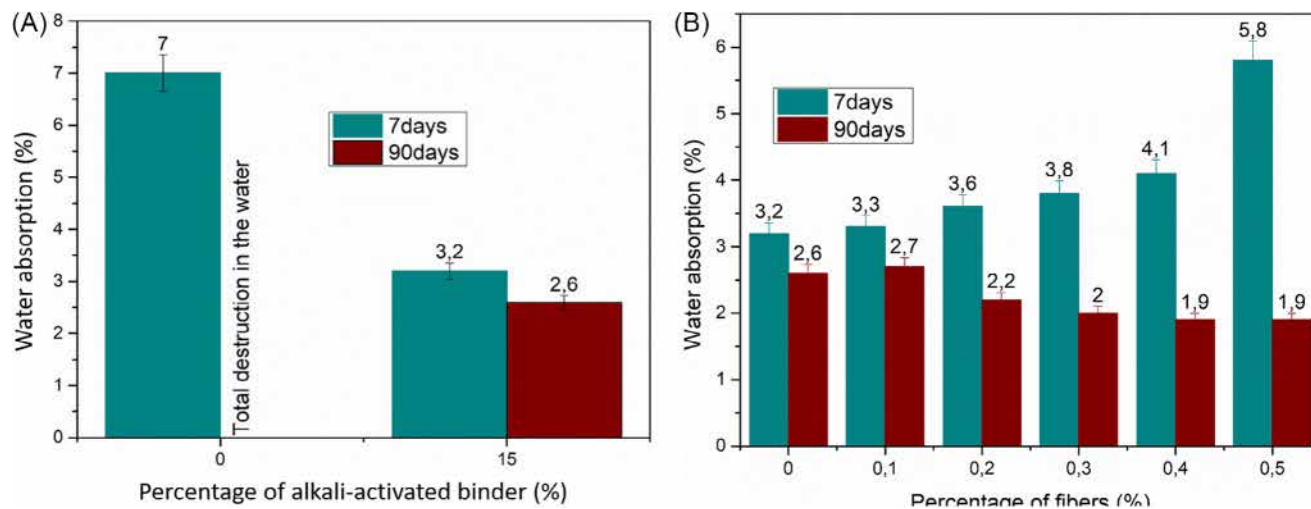


FIGURE 7 (A) Variations of water absorption with alkali-activated binder and curing time. (B) Variations of water absorption with palm fibers and curing time.

matrix, the flexural strength behavior is related to the fiber reinforcement mechanism which during the applied test was placed on the side of the stretched face.³⁵ With the addition of 0.5 wt.% fiber (drop point) and by comparing than compressive strength behavior (Figure 5B) the mechanical bending slightly dropped and remained high (Figure 6B) because the fibers participate in the seam of cracks during the bending test.³⁶ The results in Figure 7A show that, unlike the results obtained after 90 days of curing, where the variation in properties is due to the evolution of the alkali-activated binder and the addition of palm fibers, the variation in flexural strength obtained after 7 days of curing is solely due to the addition of palm fiber fractions.

3.3.4 | Water absorption

Figure 7A,B displays the trend of the water absorption of the produced CEBs. At 90 days, the produced CEB without alkali-activated binder contained more cracks within the structure and that made them vulnerable to water and therefore disintegrated completely (Figure 7A). In contrast, those stabilized with 15 wt.% of alkali-activated binder are characterized by better cohesion between binder and other components which by the end render them compact and denser. The corresponding values of the water absorption were $3.2 \pm 0.16\%$ and $2.6 \pm 0.13\%$ at 7 and 90 days, respectively. The progressive decrease observed in the water absorption rate is related to the maturation of the alkali-activated matrix, which becomes more compact over time.³⁷ In the case of the addition of the treated palm fibers (Figure 8B), the poor cohesion between the components within the matrices at 7 days induced the

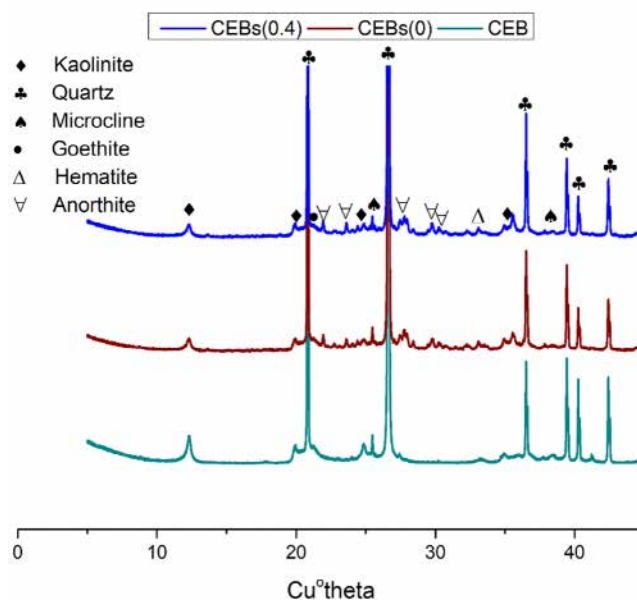


FIGURE 8 XRD of the powder of different compressed earth bricks (2θ). XRD, X-ray diffraction.

high values of the water absorption, while the hardener occurred in the further cured age at 90 days favored the decrease in absorption rate of reinforced bricks. In fact, at 7 day-aged the produced still have weak structure and this facilitating absorption of huge amount of water by fiber, which generates a high mass gain within the composite.¹⁸ According to the obtained findings, the long curing process seemed played a key factor for the development of strong bonds within the alkali-activated matrix that ensures good fiber–matrix adhesion. The present finding quite matches with statement of Fang et al.³⁸ They found that the treated fibers absorbed less water than untreated

ones, and the maturation of alkali-activated binder over the time (90 days) rendered the composites matrices more compact and reduced the absorption capacity of the fibers.

3.4 | Mineralogical characterization of composite materials

3.4.1 | X-ray diffraction analysis

Figure 8 displays the diffractogram patterns of unstabilized CEBs, stabilized CEBs with 15 wt.% of alkali-activated binder (CEBs0) and stabilized CEBs contain 0.4 wt.% of palm fiber (CEBs0.4). The phase identification shows that CEB consists the same phase identified in the clay soil: kaolinite (PDF-Nr.-000010527), quartz (PDF-Nr.-010741811), goethite (PDF-Nr.-010771060), and microcline (PDF-Nr.-000190926). CEB being made up only of CS and water, this water did not bring any modification to the mineralogy of CS. Furthermore, the addition of 15 wt.% of alkali-activated binder (natural PZ + alkaline solution) justifies the presence of new phases observed on the CEBs0 diffractogram. These new phases come from natural PZ used as the main precursor of alkaline activation reaction and correspond to: anorthite (PDF-Nr.-000411481) and hematite (PDF-Nr.-000240072). Observing the diffractogram of the sample stabilized with an alkali-activated binder and containing 0.4% of palm fiber (CEBs0.4), it noted that the addition of treated palm fibers did not cause any modification to the mineralogy of the samples. The decrease in the peaks intensity of some minerals such as kaolinite and goethite means a combination that occurs between these minerals and other phase such as activating alkaline solutions to contribute to the formation of the alkali-activated binder network, within the different composites (CEBs0 and CEBs0.4).²⁸ In addition, phases such as augite (PDF-Nr.-010781392), initially present in natural PZ are not identified in the composites (CEBs0 and CEBs0.4). This means that alkaline solution, once in contact with precursors dissolves the reactive phases to form the alkali-activated binder network.³⁹ The absence of a cellulose peak indicates that the XRD scanner did not detect any fiber content in the powdered matrix used for mineralogical characterization.

3.4.2 | Fourier transform infrared analysis

The IR spectra of the composite materials: CEB, CEBs0, and CEBs0.4 are illustrated in Figure 9. Bands located at 3623 and 3695 cm^{-1} characterized absorption bond belong to the hydroxyl (O-H) group of kaolinite.⁴⁰ The absorption

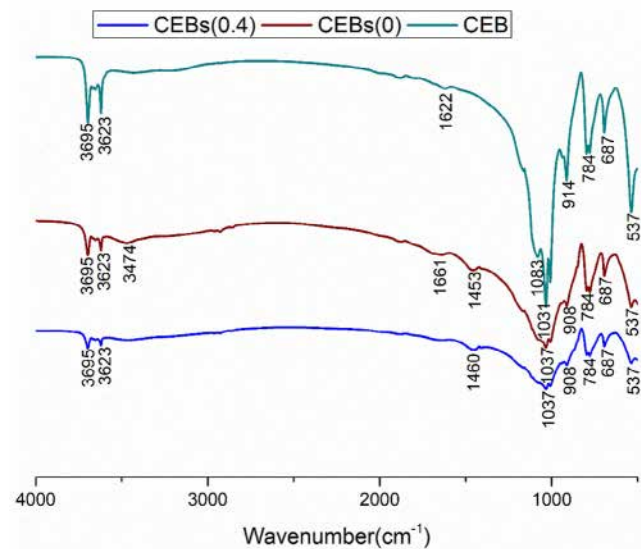


FIGURE 9 FTIR spectra of the powder of different compressed earth bricks. FTIR, Fourier transform infrared.

bond present at 3474 cm^{-1} on all IR spectra is attributed to the hydroxyl group (O-H) of water molecules.³³ The band located at 1622 cm^{-1} (CEB) and 1661 cm^{-1} (CEBs0) is described to the H-O-H bond of water molecules.⁴¹ The absence of this band on the spectrum of the sample containing 0.4 wt.% of palm fiber (CEBs0.4) reflects the sorption capacity of the water molecules of these fibers. This is consistent with the results obtained in the case of the variation in water absorption of the different samples (Section 3.3.4). The symmetrical stretching vibration bands at 908, 914, 1031, and 1083 cm^{-1} correspond to Si-O-T (T = Si, Al, Fe).⁴² The absorption band at 687 cm^{-1} characterized the bending vibration mode of Fe-OH of goethite.⁴² The decrease of this band (Fe-OH) after alkaline activation is due to the alteration of the minerals (kaolinite and goethite) present in CS.²⁸ This analysis corresponds to the observation made in Section 3.4.1. The stretching vibration absorption bands located at 537 cm^{-1} are attributed to the Fe-O-T (T = Al, Si, Fe), due to the stretching vibration bands of Fe-O.⁴² After analysis of these spectra, the main aluminosilicate band, located at 1031 and 914 cm^{-1} on the sample without stabilization (CEB), shifts respectively to 1037 and 908 cm^{-1} on stabilized brick without fiber (CEBs0) and stabilized with 0.4 wt.% of fiber (CEBs0.4) spectra. This change shows a restructuring of the aluminosilicate during the alkaline activation process, a result of the alteration of phases such as kaolinite and goethite.^{5,43} The fact that these bands shift at the same wavenumbers for the stabilized sample (CEBs0) and the stabilized sample containing 0.4% of palm fibers (CEBs0.4) reflects the fact that the treated palm fibers do not affect the alkaline activation process. This observation confirms once

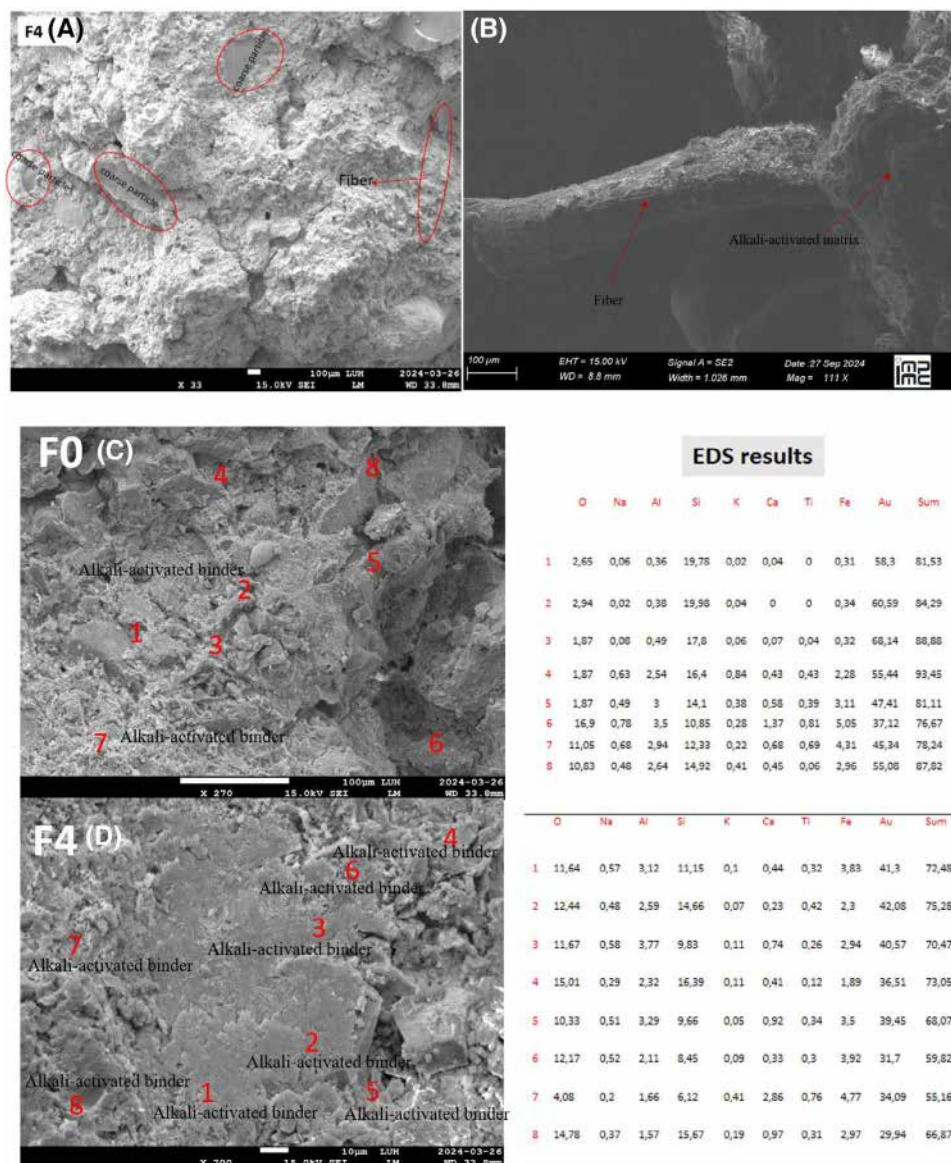


FIGURE 10 Micrographs and EDS analysis of sample. EDS, Energy dispersive X-ray spectroscopy.

again that these fibers do not deteriorate after 90 days of curing. The new bands at 1453 cm^{-1} on CEBs0 and at 1460 cm^{-1} on CEBs0.4 spectra are attributable of O–C–O bond of natrite resulting from the carbonation reaction resulting between CO_2 atmospheric and the free Na^+ ions.^{28,44}

3.4.3 | Scanning electron microscope/energy dispersive X-ray spectroscopy analysis

Figure 10 shows selected micrographs of brick residues without (F0) and with palm fibers (F4) aged at 90 days and at 1 year (F4 (b)) collected after compressive strength. The figures F0(c) and F4(d) show the adhesion between the various brick constituents, that is, the binder and coarse

non-reactive particles. F0(c) and F4(d) show that the fibers are completely embedded in the alkali-activated binder. Moreover, the fiber particle detected on the section studied (F4(a) and F4(b)) did not show any notable deterioration in the matrix after 90 days and 1 year and plays its role of reinforcement perfectly. This situation corroborates with the mechanical properties which showed an emergence of these properties with the incorporation of the fibers. Figure c,d shows high-magnification micrographs of samples without and with fibers, respectively, and aged at 90 days. The elemental chemical analyses, that is, the EDS carried out on the parts with the alkali-activated binder morphology (cloudy morphology) and the non-reactive particles, are illustrated in the tables to the right of each micrograph. This table shows that the alkali-activated binders formed consist mainly of Na, K, Si, Ca, O, Al, Si, and Fe. This

shows that the alkali-activated binder formed is a poly-ferrosialate chain commonly obtained after activation of volcanic ashes in an alkaline medium.^{32,45} The monomers of this alkali-activated binder are derived from the dissolution of certain mineralogical phases of the raw materials revealed by XRD analysis.³⁹ The presence of the Ti element comes from the chemical composition of the clay soil described in Table 1. The crystalline phases detected show no significant deterioration, confirming the fact that some particles are inert in an alkaline environment and act as aggregates in the matrix.

4 | CONCLUSION

This work focused on the study of the addition of treated palm fibers on the mechanical, mineralogical, and microstructural properties of clay bricks stabilized by an alkali-activated binder based on natural PZ. First, it has been demonstrated that the alkali-activated binder improves the physico-mechanical properties of clay bricks. Subsequently, the addition of palm fibers has enabled an optimization of these properties without affecting the geopolymerization reaction during which there is formation of the alkaline binder network that ensures the fiber-matrix adhesion of the composite formed. The X-ray and FTIR analyses of the 90-day-old matrices indicated that certain mineralogical phases of the raw materials dissolve during alkaline activation. Moreover, the observation of the micrographs and EDS of the selected samples revealed that the treated palm fibers remained undecomposed in the alkaline activated matrix at 90 days and 1 year of age.

This work demonstrates thus the potential of these composite materials (alkali-activated brick-treated palm fiber) to be used as sustainable construction materials for building houses in tropical areas. However, an additional of 0.4 wt.% of the treated palm fibers in earth bricks stabilized by the alkali-activated binder-based natural PZ is recommended to achieve a composite brick with good physical and mechanical performance. In prospect, investigation focused on the detailed evolution morphology of the complete profiles of all samples reinforced with 0 up to 0.5 wt.% of the palm fiber and the durability of the resulting composites as well will be carried out.

ACKNOWLEDGMENTS

The authors thank LASOGEMA (IUT-Douala-Cameroon), IRD ERL 206 and IMPMC France for extending all the facilities to carry out this research.

CONFLICT OF INTEREST STATEMENT


The authors declare no conflicts of interest.

FUNDING INFORMATION

The authors of manuscript did not receive any funding and grants for this work.

ORCID

Rolande Aurelie Tchouateu Kamwa  <https://orcid.org/0000-0001-9695-1123>

Juvenal Giogetti Deutou Nemaleu  <https://orcid.org/0000-0002-3249-3159>

REFERENCES

- Ghadir P, Ranjbar N. Clayey soil stabilization using geopolymer and Portland cement. *Constr Build Mater*. 2018;188:361–71.
- Oti JE, Kinuthia JM. The development of stabilised clay-hemp building material for sustainability and low carbon use. *J Civil Eng Constr*. 2020;9:205–14.
- Dime T, Sore SO, Nshimiyimana P, Messan A, Courard L. Comparative study of the reactivity of clay earth materials for the production of compressed earth blocks in ambient conditions: effect on their physico-mechanical performances. *J Min Mater Charact Eng*. 2022;10:43–56.
- Tung LH, Khadraoui F, Boutouil M, Gomina M. Characterizations mechanical and microstructural of flax fibre cement composite reinforced | Caractérisation microstructurale et mécanique d'un composite cimentaire renforcé par des fibres de lin. *MATEC Web of Conferences*. 2012. P. 2.
- Aurelie R, Tome S, Nemaleu JGD, Noubissie LT, Tommes B, Eguekeng I, et al. Effect of curing temperature on properties of compressed lateritic earth bricks stabilized with natural pozzolan-based geopolymer binders synthesized in acidic and alkaline media. *Arab J Sci Eng*. 2023;48:16151–65. <https://doi.org/10.1007/s13369-023-08069-0>
- Aurelie R, Tome S, Chongouang J, Eguekeng I, Spieß A, Fetzner MNA, et al. Stabilization of compressed earth blocks (CEB) by pozzolana based phosphate geopolymer binder: physico-mechanical and microstructural investigations. *Clean Mater*. 2022;4:100062.
- Djobo JNY, Tome S. Insights into alkali and acid-activated volcanic ash-based materials: a review. *Cem Concr Compos*. 2024;152:105660.
- Majidi Behzad. Geopolymer technology, from fundamentals to advanced applications: a review. *Materials Technology Advanced Performance Materials*. 19 Jul 2013 <https://doi.org/10.1179/175355509x449355>
- Koadri Z, Benyahia A, Deghfel N, Belmokre K, Nouibat B, Redjem A. Étude de l'effet du temps de traitement alcalin de fibres palmier sur le comportement mécanique des matériaux à base d'argile rouge de la région de M'sila. *Mater Tech*. 2019;107:404.
- Syed M, Guharay A, Goel D. Strength characterisation of fiber reinforced expansive subgrade soil stabilized with alkali activated binder. 2021. *journal/Road-Materials-and-Pavement-Design-2164-7402* <https://doi.org/10.1080/14680629.2020.1869062>
- Hoyle D, Levang P. Le développement du palmier à huile au Cameroun. WWF, IRD, CIFOR; 2012. p. 16.

12. Adazabra AN, Viruthagiri G, Foli BY. Evaluating the technological properties of fired clay bricks incorporated with palm kernel shell. *J Build Eng*. 2023;72:106673.
13. Kadir AA, Sarani NA, Abdullah MMAB, Perju MC, Sandu AV. Study on fired clay bricks by replacing clay with palm oil waste: effects on physical and mechanical properties. *IOP Conference Series: Materials Science and Engineering*. IOP; 2017. p. 209.
14. Kamwa RAT, Tome S, Chongouang J, Eguekeng I, Spieß A, Fetzner MNA, et al. Stabilization of compressed earth blocks (CEB) by pozzolana based phosphate geopolymer: physico-mechanical, structural and microstructural investigations. *Clean Mater*. 2022;4:1–22.
15. Ali A, Shaker K, Nawab Y, Jabbar M, Hussain T, Militky J, Baheti V. Hydrophobic treatment of natural fibers and their composites—a review. *J Ind Text*. 2018;47:2153–83.
16. Manniello C, Cillis G, Statuto D, Di A, Picuno P. Appliqué sciences Blocs en bé ton renforcés par des fibres naturelles d ' Arundo donax avec diff é rents rapports d ' aspect pour une application en bioarchitecture. *Appl Sci*. 2022;12(4), 2167. <https://doi.org/10.3390/app12042167>
17. Sharma V, Vinayak HK, Marwaha BM. Enhancing sustainability of rural adobe houses of hills by addition of vernacular fiber reinforcement. *Int J Sustain Built Environ*. 2015;4:348–58.
18. Elfaleh I, Abbassi F, Habibi M, Ahmad F, Guedri M, Nasri M, Garnier C. A comprehensive review of natural fibers and their composites: an eco-friendly alternative to conventional materials. *Results Eng*. 2023;19:101271.
19. Nana A, Kamseu E, Akono A-T, Ngouné J, Yankwa Djobo JN, Tchakouté HK, et al. Particles size and distribution on the improvement of the mechanical performance of high strength solid solution based inorganic polymer composites: a microstructural approach. *Mater Chem Phys*. 2021;267:124602.
20. Onyelowe KC, Tome S, Ebid AM, Usungedo T, Bui Van D, Etim RK, et al. Effect of desiccation on ashcrete (HSDA) -treated soft soil used as flexible pavement foundation: zero carbon stabilizer approach. *Int J Low-Carbon Technol*. 2022;17:563–70. <https://doi.org/10.1093/ijlct/ctac042>
21. Guggenheim S, Alietti A, Drits VA, Formoso MLL, Galán E, Köster HM, et al. Report of the Association Internationale Pour l'Étude des Argiles (Aipea) Nomenclature Committee for 1996. *Clays Clay Miner*. 1997;45:298–300.
22. Ouedraogo E, Coulibaly O, Ouedraogo A, Messan A. Mechanical and thermophysical properties of cement and / or paper (cellulose) stabilized compressed clay bricks. *J Mater Eng Struct*. 2015;2:68–76.
23. Zuluaga R, Putaux JL, Cruz J, Vélez J, Mondragon I, Gañán P, et al. Cellulose microfibrils from banana rachis: effect of alkaline treatments on structural and morphological features. *Carbohydr Polym*. 2009;76:51–59.
24. Christine DA, Séraphin DA, Olivier BM, Edjikémé E. Effet de l'addition de fibres de coco traitées à la potasse sur les propriétés mécaniques des matériaux de construction à base d'argile – ciment. *Eur Sci J*. 2018;14:104–16.
25. Abdelhak M, Fazia F, Abdelmadjid H. Effet des traitements des fibres de palmier dattier sur le comportement mécanique de l ' interface fibre-matrice de terre stabilisée. *RUGC 2020 AJCE*. 2020;38(1):73–76.
26. Malanda N, Louzolo-kimbembe P, Tamba-nsemi YD. Etude des caractéristiques mécaniques d ' une brique en terre stabilisée à l ' aide de la mélasse de canne à sucre. *Revue RAMReS Sci Appl Ing*. 2018;2:1–9.
27. Benmansour N. Développement et caractérisation de composites naturels locaux adaptés à l'isolation thermique dans l'habitat. 2015;162. <http://dspace.univ-batna.dz/xmlui/handle/123456789/747>
28. Tome S, Shikuku V, Tamaguelon HD, Akiri S, Etoh MA, Rüscher C, et al. Efficient sequestration of malachite green in aqueous solution by laterite-rice husk ash-based alkali-activated materials: parameters and mechanism. *Environ Sci Pollut Res*. 2023;30:67263–77. <https://doi.org/10.1007/s11356-023-27138-3>
29. Mousi JB, Aurelie TKR, Nemaleu JGD, Tome S, Gerard M, Etoh M-A, et al. Improvement of the bearing capacity of lateritic gravel by a geopolymer binder: road construction in tropical countries. *Innov Infrastruct Solut*. 2024;9:242.
30. Kemp SJ, Gillespie MR, Leslie GA, Zwingmann H, Campbell SDG. Clay mineral dating of displacement on the Sron-lairig fault: implications for Mesozoic and Cenozoic tectonic evolution in northern Scotland. *Clay Miner*. 2019;54:181–96.
31. Debieb SKF. Characterization of the durability of recycled concretes using coarse and fine crushed bricks and concrete aggregates. *Mater Struct*. 2011;44(4):815–24. <https://doi.org/10.1617/s11527-010-9668-7>
32. Tome S, Etoh M-A, Etame J, Kumar S. Improved reactivity of volcanic ash using municipal solid incinerator fly ash for alkali-activated cement synthesis. *Waste Biomass Valorization*. 2020;11:3035–44.
33. Tome S, et al. Resistance of alkali-activated blended volcanic ash-MSWI-FA mortar in sulphuric acid and artificial seawater. *Silicon*. April 2021;14(6). <https://doi.org/10.1007/s12633-021-01055-x>
34. Kaze RC, Beleuk À Mounkam LM, Fonkwe Djouka ML, Nana A, Kamseu E, Chinje Melo UF, et al. The corrosion of kaolinite by iron minerals and the effects on geopolymerization. *Appl Clay Sci*. 2017;138:48–62.
35. Nematollahi B, Sanjayan J, Chai JXH, Lu TM. Properties of fresh and hardened glass fiber reinforced fly ash based geopolymer concrete. *Key Eng Mater*. 2014;594–595:629–33.
36. Matthieu, MS. Potentiel des fibres végétales courtes dans l'amélioration du comportement mécanique des mortiers. 2022. <https://theses.hal.science/tel-03772550>
37. Criado M, Aperador W, Sobrados I. Microstructural and mechanical properties of alkali activated Colombian raw materials. *Materials*. 2016;9:158.
38. Wen Fang T, Nur Asyikin NSS, Abdul Khalil HPS, Mohamad Kassim MH, Syakir MI. Water absorption and thickness swelling of oil palm empty fruit bunch (OPEFB) and seaweed composite for soil erosion mitigation. *J Phys Sci*. 2017;28: 1–17.
39. Tome S, Nana A, Tchakouté HK, Temuujin J, Rüscher CH. Mineralogical evolution of raw materials transformed to geopolymer materials: a review. *Ceram Int*. 2024;50:35855–68. <https://doi.org/10.1016/j.ceramint.2024.07.024>
40. Ramadji C, Messan A, Sore SO, Prud'Homme E, Nshimiymana P. Microstructural analysis of the reactivity parameters of calcined clays. *Sustainability*. 2022;14:2308.
41. Tome S, Bewa CN, Nana A, Deutou Nemaleu JG, Etoh MA, Tchakouté HK, et al. Structural and physico-mechanical

- investigations of mine tailing-calcined kaolinite based phosphate geopolymer binder. *Silicon*. 2022;14:3563–70.
42. Kaze RC, Mounsam LMB, Cannia M, Rosa R, Kamseu E, Melo UC, et al. Microstructure and engineering properties of $\text{Fe}_2\text{O}_3(\text{FeO})\text{-Al}_2\text{O}_3\text{-SiO}_2$ based geopolymer composites. *J Cleaner Prod*. 2018;199:849–59.
43. Tome S, Annie M, Jacques E, Sanjay E. Improved reactivity of volcanic ash using municipal solid incinerator fly ash for alkali-activated cement synthesis. *Waste Biomass Valorization*. 2019;11:3035–44.
44. Aurelie Tchouateu Kamwa R, Tchadjie Noumbissie L, Tome S, Idriss E, Giogetti Deutou Nemaleu J, Tommes B, et al. A comparative study of compressed lateritic earth bricks stabilized with natural pozzolan-based geopolymer binders synthesized in acidic and alkaline conditions. *Constr Build Mater*. 2023;400:132652.
45. Djobo JNY, Elimbi A, Tchakouté HK, Kumar S. Reactivity of volcanic ash in alkaline medium, microstructural and strength characteristics of resulting geopolymers under different synthesis conditions. *J Mater Sci*. 2016;51:10301–17. <https://doi.org/10.1007/s10853-016-0257-1>

How to cite this article: Kamwa RAT, Mousi JB, Tome S, Nemaleu JGD, Gérard M, Etoh M-A, et al. Effect of treated palm fibers on the mechanical properties of compressed earth bricks stabilized by alkali-activated binder-based natural pozzolan. *Int J Ceramic Eng Sci*. 2025;7:e10246. <https://doi.org/10.1002/ces2.10246>